NJC

PAPER

Cite this: *New J. Chem.*, 2018, **42**, 2605

Broadband dielectric spectroscopy of micelles and microemulsions formed in a hydrophilic ionic liquid: the relaxation mechanism and interior parameters†

Yiwei Lian[b] and Kongshuang Zhao *[a]

Three striking dielectric relaxations located at 100 MHz, 1 GHz and 10 GHz respectively were observed both in binary mixtures of *p*-(1,1,3,3-tetramethylbutyl)phenoxypolyoxyethyleneglycol (TX-100) and 1-butyl-3-methylimidazolium tetrafluoroborate ([bmim][BF_4]), and in [bmim][BF_4]/TX-100/cyclohexane microemulsions in a wide frequency range. The mechanisms of the dielectric relaxations were proposed and the detailed characterization of low-frequency relaxation (around 100 MHz), which is identified as interface polarization, was performed theoretically. The dielectric parameters (relaxation time and dielectric increment) were obtained by fitting the dielectric spectra with the Debye plus cole–cole formula. The low-frequency relaxation mechanisms of both binary and ternary systems contribute to interfacial polarization, supported by the good agreement between relaxation times calculated by Maxwell–Wagner theory and the values obtained from experiment. Meanwhile, by analyzing the linear ionic liquid content dependence of dielectric increment of low-frequency relaxation, we find that this relaxation involves the dynamics of ionic liquids which located at the interface. Besides, the phase parameters, which reflect the interior properties of the binary and ternary systems, were calculated by Hanai theory, and their dependence on the variation of sample composition are properly explained; the distribution of cyclohexane in the dispersed phase is obtained quantitatively, which is of importance in the field of the microstructure of ionic liquid microemulsions.

Received 6th December 2017,
Accepted 4th January 2018

DOI: 10.1039/c7nj04813k

rsc.li/njc

1. Introduction

The molecular self-organization systems of surfactant molecules formed within ionic liquids (ILs), such as micelles[1–6] and microemulsions,[7–22] as a class of important soft matter, are attracting increasing interest. This is because these aggregations can not only overcome solubility limitations of ILs in immiscible solvents but also provide hydrophobic or hydrophilic nanodomains,[3,7] *i.e.* they gather the advantages of both ILs and self-association, thereby expanding applications of ILs in micro-heterogeneous systems as reaction, separation and extraction media.[12] The non-volatility of ILs makes these systems contribute much to green chemistry.[23] Moreover, the most promising fact about IL-in-oil microemulsions is their high thermal stability compared to that of aqueous microemulsions.[21] The above reasons are considered from the perspective of applications. In fundamental research, these systems can provide a special model for studying the characteristics of soft matter, such as molecular interactions, scaling laws, dynamics *etc.* This is because coulomb, hydrophobic and hydrophilic interactions exist widely in these systems, leading to their distinctive features different from traditional micelles, microemulsions and other molecular self-organization systems.

Thus, several groups have prepared and characterized IL micelles and microemulsions by using a variety of techniques, recently.[1–18,20–22] The aggregation behavior of a class of non-ionic surfactants in 1-butyl-3-methylimidazolium ([bmim]$^+$) type ILs with various counterions was researched by Lauth-Viguerie *et al.*[2] Greaves and Drummond published a review which includes critical micellar concentrations (CMCs) of surfactants in ILs.[6] Zheng *et al.*[4] studied the micelles of *p*-(1,1,3,3-tetramethylbutyl)phenoxypolyoxyethyleneglycol (TX-100, a non-ionic surfactant with a polyoxyethylene (PEO) chain) formed within 1-butyl-3-methylimidazolium tetrafluoroborate ([bmim][BF_4]) and 1-butyl-3-methylimidazolium hexafluorophosphate ([bmim][PF_6]) using two-dimensional rotating frame nuclear Overhauser effect experiments and ^{1}H NMR, and they found that the addition of TX-100 destroyed the ion pairs of pure ILs due to the electrostatic interactions between electronegative

[a] *College of Chemistry, Beijing Normal University, Beijing 100875, China. E-mail: zhaoks@bnu.edu.cn; Tel: +8601058805856*
[b] *Key Laboratory for Resource Exploration Research of Hebei Province, College of Materials Science and Engineering, Hebei University of Engineering, Handan, Hebei, 056038, China*

† Electronic supplementary information (ESI) available. See DOI: 10.1039/c7nj04813k

oxygen atoms of oxyethylene (OE) units of TX-100 and positively charged imidazolium cations of the ILs.

The microemulsions with ILs as nano-sized domains have been intensively studied.[7–18] In these studies, for microemulsions with ILs acting as the non-polar phase the hydrophobic IL [bmim][PF_6] is the most used.[15–18] On the other hand, for preparation and characterization of microemulsions for which ILs serve as the polar phase, hydrophilic [bmim][BF_4][7,9–14] is used widely. The information obtained from these studies includes: the phase behavior,[7,9–14] the shape and size of the droplets,[7] the structure of the microemulsion,[9,12,14] the effect of a compressed gas on the properties of IL microemulsions,[8] the sub-regions of IL microemulsions and the transition structure between them,[7,9–11,15] the interaction between different species,[11] the effect of water on IL-in-oil (IL/O) microemulsions[14] *etc.* At the same time, several reports indicated that IL/O and IL/W microemulsions have potential applications in the production of metallic or semiconductor nanomaterials, and in biological extractions or as solvents for enzymatic reactions.[10,24–26] Sarkar *et al.* even prepared high-temperature stable IL-in-oil microemulsions and demonstrated the wide range of thermal stability of these IL microemulsions.[21]

Although considerable research studies on the microstructure of ionic liquid micelles/microemulsions have been performed, there still remain unsolved problems. One of them is that the individual electrical properties of the constituent phase, such as permittivity and conductivity of continuous and dispersed phases, as far as we know, are not reported. Some phenomena, such as the addition of TX-100 destroys ion pairs of ILs,[4] the CMCs of TX-100 in ILs are relatively high,[4] a large quantity of TX-100 is added in order to get stable IL microemulsions,[7] the insertion of ILs into the TX-100 micelle phase[19] and the interface palisade layer of microemulsions[9] will strongly affect the permittivity and conductivity of the continuous and dispersed phases. Furthermore, the volume fractions of dispersed phases (micelles, IL-in-oil and oil-in-IL microdroplets) in the continuous phase, cyclohexane in oil-in-IL (O/IL) droplets have not been quantitatively described still. And more importantly, the mechanisms of different interactions in these systems are also not clear.

As a method to obtain the internal electrical and structural properties of the constituent phases, dielectric relaxation spectroscopy (DRS) is probably a suitable technology to research the above problems, because it is a powerful method to determine precise relaxation times of polarization in self-organization systems in a wide frequency range. From the low dielectric relaxation (1–100 kHz), one can study the interface polarization in both micelle[27–29] and microemulsion systems.[30,31] Using phase parameters obtained theoretically by analyzing the dielectric spectral data from dielectric measurements, the distribution of cosurfactants in constituent phases, which is of importance in the field of the microstructure of microemulsions, can be obtained quantitatively.[32]

Recently, systematic dielectric studies of pure ILs have been reported by Weingärtner,[33] Buchner,[34] Nakamura[35] *etc.* Only a few reports involve the dielectric methods on binary or ternary mixtures of ILs. Such as, Buchner *et al.*[36] studied the dielectric spectra of [bmim][BF_4]/DCM (dichloromethane) mixtures and indicated that the IL appears to retain its chemical character to extraordinarily high levels of dilution in DCM. They also reported the dielectric behavior of binary mixtures of [bmim][BF_4][37] and the collaborative rotation and translational motion of each species in the mixtures. Licence *et al.*[38] discussed the influence of water on the dielectric properties of ILs and identified the formation of a water dimer. Apart from the above mentioned studies, the dielectric data of molecular self-organization systems composed of surfactants and ILs have been reported in our previous publications,[39,40] but we only had space to discuss the interaction, percolation, solution, and softness of these systems, because the information obtained from our measurement is too rich to be included in one paper.

Relative to our series of work for the dielectric analysis of micelles and microemulsions formed in a hydrophilic ionic liquid [bmim][BF_4],[39] in this paper, based on the measured dielectric spectra of the broadband frequency range, we will discuss the polarization mechanism of low-frequency relaxation and the internal properties of the constituent phase.

2. Experimental and methods

2.1. Preparation of IL-based micelles and microemulsions

The IL [bmim][BF_4] (purity > 99%) was purchased from Shanghai Cheng Jie Chemical Co. Ltd, China. TX-100(*p*-(1,1,3,3-tetramethylbutyl)phenoxypolyoxyethyleneglycol) (reagent grade) was obtained from Amresco Chemical Inc, America. Cyclohexane was produced by Beijing Chemical Reagent Factory, China. The structures of the IL and the surfactant are shown in Chart 1, they were dried under vacuum at 80 °C for 12 h to remove excess water before use.

TX-100 was dissolved with [bmim][BF_4] at TX-100 concentration ranges from 0 to 100 wt%. The microemulsions were prepared by mixing appropriate weight fractions of [bmim][BF_4], TX-100, and cyclohexane. The experimental paths are shown in the insets of Fig. 1. The details of preparing the IL-based micelles and microemulsions were reported in our previous work.[39]

2.2. Dielectric measurements

The dielectric spectra were obtained by the combined use of two instruments. The low-frequency dielectric measurements were carried out on a 4294A Precision Impedance Analyzer from Agilent Technologies (Made in Japan) that allows continuous frequency measurements from 40 Hz to 110 MHz. A dielectric measurement cell with concentric cylindrical platinum electrodes

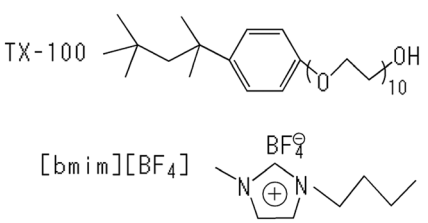

Chart 1 The chemical structures of TX-100 and [bmim][BF_4].

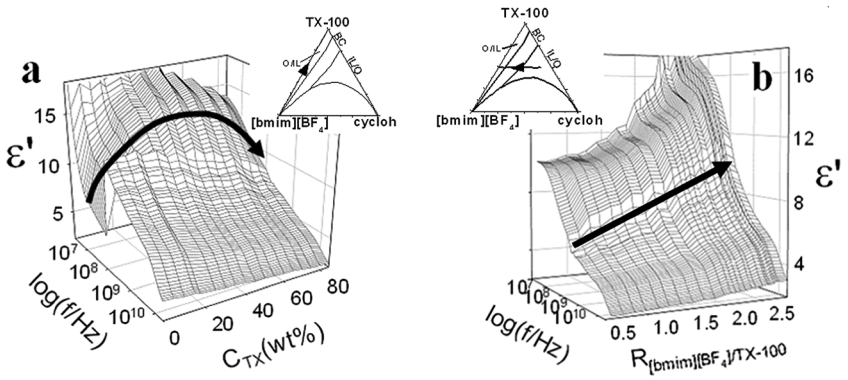

Fig. 1 Three-dimensional representations for the frequency dependencies of permittivity ($\varepsilon'(\omega)$) of (a) [bmim][BF_4]/TX-100 binary systems with different weight concentrations of TX-100 (C_{TX}) and (b) [bmim][BF_4]/TX-100/cyclohexane ternary systems (when the weight fraction of TX-100 is fixed as 50 wt%) with different IL/TX-100 molar ratios ($R_{[bmim][BF4]/TX-100}$). For clarity, corresponding experimental paths of the above two systems are shown as insets in this figure.

and a circulating water set was employed, and connected to the impendence analyzer by means of a 1607E Spring Clip fixture (Agilent Technologies, made in Japan). The cell constant and stray capacitance were determined by using air, pure ethanol and pure water. The correction of measured dielectric data was introduced in ref. 40.

The high-frequency dielectric spectra were measured using an Agilent E8362B PNA Series Network Analyzer (Agilent Technologies, Made in America), equipped with an Agilent 85070E open-ended coaxial probe (Agilent Technologies, Made in America), covering the frequency range from 10 MHz to 20 GHz. The probe was immersed into the liquid material. The fields at the probe end ''fringe'' into the material and change as they come into contact with the material under test. The reflected signal (S11) can be measured and used to calculate the complex permittivity ε^*.[41] Permittivity and total dielectric loss were automatically calculated as a function of frequency by the built-in software of this measuring system. Both the measuring systems were tested and calibrated in accordance with the procedures recommended by the manufacturers, respectively. In order to solve for possible errors, three well-known standards are measured. The difference between the predicted and actual values is used to remove the systematic (repeatable) errors from the measurement. The three known standards are air, a short circuit, and distilled and de-ionized water. The dielectric measurements for binary systems and ternary mixtures were conducted at 25 ± 0.1 °C and 35 ± 0.1 °C, respectively.

2.3 Determination of dielectric parameters

In an applied electric field of angular frequency ω, the dielectric properties of samples can be characterized by ε^*, which is defined as

$$\varepsilon^*(\omega) = \varepsilon'(\omega) - j\varepsilon''(\omega) \quad (1)$$

where $\varepsilon'(\omega)$ and $\varepsilon''(\omega)$ are the permittivity and dielectric loss, respectively. It was found that a superposition of three relaxation processes is required for a consistent fit of all the spectra of the binary and ternary mixtures, they can be characterized by a set of dielectric parameters which can be obtained by fitting the empirical function with two cole–cole relaxation terms and one Debye relaxation term to the experimental data:[42]

$$\varepsilon^*(\omega) = \varepsilon_h + \frac{\Delta\varepsilon_l}{1+(j\omega\tau_l)^{\alpha_l}} + \frac{\Delta\varepsilon_m}{1+(j\omega\tau_m)^{\alpha_m}} + \frac{\Delta\varepsilon_h}{1+j\omega\tau_h} \quad (2)$$

where ε_h is the high-frequency limit of permittivity, $\Delta\varepsilon$ and τ are the dielectric increment and the relaxation time, respectively; α ($0 < \alpha \leq 1$) is the parameters related to the distribution of the relaxation time; subscripts l, m and h denote low-(around 100 MHz), mid-(around 1 GHz) and high-(around 10 GHz) frequency relaxation, respectively.

2.4 Calculation of phase parameters

While relaxation parameters represent the collective properties of a micelle/microemulsion system, phase parameters represent the individual electrical properties of the constituent phase, such as the permittivity and conductivity of the two phases, and the volume fraction occupied by the dispersed phase. For the sake of simplicity in modeling the microstructures of micelles, IL/O and O/IL nano-sized domains were formed in the IL and we suppose that they are spherical droplets dispersed in a continuous phase. As an extension of Wagner's equation[43] to high volume fractions along the Bruggeman's[44] effective medium approach, the Hanai theory[45–47] can be expressed as

$$\frac{\varepsilon^* - \varepsilon_i^*}{\varepsilon_a^* - \varepsilon_i^*}\left(\frac{\varepsilon_a^*}{\varepsilon^*}\right)^{1/3} = 1 - P \quad (3)$$

On the basis of this equation, the formulae related to the limiting values of low- and high-frequencies are given by

$$\frac{\varepsilon_h - \varepsilon_i}{\varepsilon_a - \varepsilon_i}\left(\frac{\varepsilon_a}{\varepsilon_h}\right)^{1/3} = 1 - P \quad (4)$$

$$\varepsilon_l\left(\frac{3}{\kappa_l - \kappa_i} - \frac{1}{\kappa_l}\right) = 3\left(\frac{\varepsilon_a - \varepsilon_i}{\kappa_a - \kappa_i} + \frac{\varepsilon_i}{\kappa_l - \kappa_i}\right) - \frac{\varepsilon_a}{\kappa_a} \quad (5)$$

$$\kappa_h\left(\frac{3}{\varepsilon_h - \varepsilon_i} - \frac{1}{\varepsilon_h}\right) = 3\left(\frac{\kappa_a - \kappa_l}{\varepsilon_a - \varepsilon_i} + \frac{\kappa_l}{\varepsilon_h - \varepsilon_i}\right) - \frac{\kappa_a}{\varepsilon_a} \quad (6)$$

$$\frac{\kappa_l - \kappa_i}{\kappa_a - \kappa_i}\left(\frac{\kappa_a}{\kappa_l}\right)^{1/3} = 1 - P \quad (7)$$

where P is the volume fraction of the dispersed phase, and subscripts a and i denote the continuous medium and the dispersed phase, respectively. After cumbersome mathematical treatments, the phase parameters (ε_i, κ_i, κ_a and P) are approximately estimated from the dielectric parameters. ε_a is considered a constant at a constant temperature. By using the phase parameters, the expression of the relaxation time in Maxwell–Wagner theory of interfacial polarization can be calculated by

$$\tau_{MW} = \frac{2\varepsilon_a + \varepsilon_i + P(\varepsilon_a - \varepsilon_i)}{2\kappa_a + \kappa_i + P(\kappa_a - \kappa_i)}\varepsilon_0 \quad (8)$$

3. Results

Fig. 1a and b show the frequency dependencies of permittivity of [bmim][BF_4]/TX-100 micelles with different C_{TX} and [bmim][BF_4]/TX-100/cyclohexane microemulsions with different $R_{[bmim][BF4]/TX-100}$ when the weight fraction of TX-100 is fixed as 50 wt%. In order to facilitate understanding, the corresponding experimental paths of the above two systems are also involved in Fig. 1 as the inset. It is obvious that from the figure at least two dielectric relaxations around 100 MHz and 10 GHz can be observed, and the dielectric spectra changed obviously with the change of the mixture composition.

Fig. 2 shows the comparison between the dielectric spectra, $\varepsilon''(\omega)$ (plane above) and $\varepsilon'(\omega)$ (plane below), of the pure IL, pure TX-100, the [bmim][BF_4]/TX-100 binary mixture and the [bmim][BF_4]/TX-100/cyclohexane ternary system. Several dielectric relaxations are observed not only in the pure substance, but also in the mixture systems. It can be seen from Fig. 3 that there exist only two dielectric relaxations in both the pure systems. Once the IL and TX-100 are mixed, another relaxation which is located in the lowest frequency range appears, and the frequency dependence of permittivity of the original two dielectric relaxations is between that of the pure IL and TX-100; when

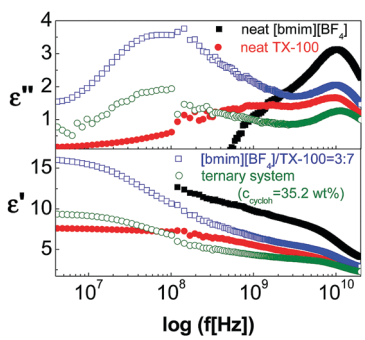

Fig. 2 The frequency dependence of dielectric loss ($\varepsilon''(\omega)$) (plane above) and $\varepsilon'(\omega)$ (plane below) of pure [bmim][BF_4] (■), pure TX-100 (●), [bmim][BF_4]/TX-100 binary systems (□) whose weight ratio is 3 : 7, and the [bmim][BF_4]/TX-100/cyclohexane ternary system (○) in which the weight concentration of cyclohexane is 35.2 wt% and the weight ratio of IL/TX-100 is 3 : 7.

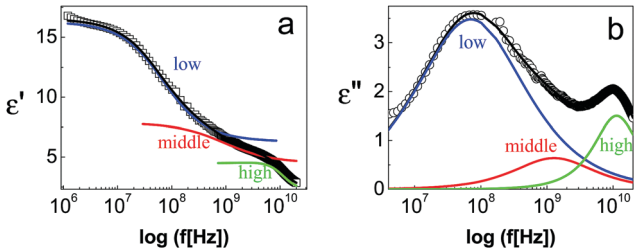

Fig. 3 Comparison between the experimental data (□) $\varepsilon'(\omega)$, (○) $\varepsilon''(\omega)$ of the [bmim][BF_4]/TX-100 binary system (when the weight ratio is 3 : 7) and the fitting curves (the black solid lines). The colored solid lines represent the fitting results of low-, mid- and high-frequency relaxations, respectively.

cyclohexane is added to the [bmim][BF_4]/TX-100 mixtures, the three dielectric relaxations are all changed and the frequency dependences of $\varepsilon'(\omega)$ of the two dielectric relaxations appearing in the pure systems are both below that of pure TX-100.

Eqn (2) was used to fit the experimental dielectric data of pure substances and mixtures, respectively, and the fitting curves are in good agreement with the experimental data as shown in Fig. 3 for example, where the symbols represent the experimental data of the [bmim][BF_4]/TX-100 binary system when their weight ratio is 3 : 7, the black solid lines represent the best fitting curves evaluated from eqn (2). The colored solid lines are the fitting results of first, second and third term of eqn (2), respectively. Thus, the dielectric parameters of every sample are obtained and shown in Table 1 and Fig. 4–6. The dielectric parameters are determined by the internal micro-mechanism of these systems; therefore, the dielectric parameters of low-frequency relaxation will be analyzed in the following section in order to get the polarization information of the IL-based micelles and microemulsions.

4. Discussion

4.1 Dielectric parameters of the pure substance

It can be seen in Table 1 that for the pure [bmim][BF_4] system, low-frequency limits (ε_l) of permittivity, dielectric increment ($\Delta\varepsilon_h$) and relaxation time (τ_m) of the mid-frequency relaxation are in good agreement with the literature,[34,35] maybe the little difference is because they are from different samples. Meanwhile, the values of ε_l of pure TX-100 are also obtained by the fitting as shown in Table 1. Specially, ε_l of the pure IL and TX-100 (which is also static permittivity of these systems) will be used as the permittivity of the continuous phase to estimate the phase parameters which will be discussed in the following sections.

4.2 Low-frequency relaxation mechanism and phase parameters of IL-based micelles

It can be seen in Fig. 4a, 5a and 6a that the values of τ_l (experimental value) and τ_{MW} (theoretical value) of every sample are not only close to each other, but also have the same concentration dependence trend. Considering that TX-100 micelles in [bmim][BF_4] have formed because the smallest

Table 1 Dielectric parameters of the pure system and [bmim][BF_4]/TX-100 binary mixtures obtained by fitting the dielectric spectra with eqn (2). The fitting errors are between 2–3%

C_{TX} (wt%)	ε_l	$\Delta\varepsilon_l$	τ_l (ns)	$\Delta\varepsilon_m$	τ_m (ps)	$\Delta\varepsilon_h$	τ_h (ps)	ε_h
0	13.06	—	—	6.4 ± 0.1	170 ± 4	3.53 ± 0.09	14.4 ± 0.4	3.12 ± 0.08
25.0	22.38	13.0 ± 0.3	1.10 ± 0.03	3.3 ± 0.1	144 ± 4	3.21 ± 0.08	13.9 ± 0.4	2.88 ± 0.08
30.1	20.83	12.6 ± 0.3	1.28 ± 0.03	2.31 ± 0.07	128 ± 4	3.12 ± 0.08	13.7 ± 0.3	2.80 ± 0.08
35.0	19.76	12.0 ± 0.3	1.43 ± 0.04	2.08 ± 0.06	120 ± 3	2.94 ± 0.07	13.6 ± 0.3	2.79 ± 0.07
40.0	18.72	11.5 ± 0.3	1.58 ± 0.04	1.66 ± 0.05	112 ± 3	2.83 ± 0.07	13.55 ± 0.3	2.76 ± 0.07
44.9	17.87	10.9 ± 0.3	1.67 ± 0.05	1.50 ± 0.04	110 ± 3	2.75 ± 0.06	13.5 ± 0.3	2.69 ± 0.07
50.1	17.51	10.7 ± 0.3	1.80 ± 0.05	1.57 ± 0.04	114 ± 3	2.68 ± 0.06	13.6 ± 0.3	2.55 ± 0.07
54.9	16.95	10.1 ± 0.3	1.93 ± 0.05	1.64 ± 0.04	122 ± 3	2.63 ± 0.06	13.6 ± 0.3	2.56 ± 0.07
60.0	16.96	9.9 ± 0.3	1.94 ± 0.05	2.06 ± 0.05	123 ± 3	2.54 ± 0.06	13.7 ± 0.3	2.49 ± 0.06
65.1	16.51	9.4 ± 0.3	2.25 ± 0.06	2.28 ± 0.06	127 ± 3	2.38 ± 0.06	13.8 ± 0.3	2.45 ± 0.06
70.0	16.24	8.9 ± 0.3	2.40 ± 0.07	2.67 ± 0.06	129 ± 3	2.31 ± 0.06	13.8 ± 0.3	2.37 ± 0.06
75.0	15.93	8.6 ± 0.3	2.55 ± 0.07	2.79 ± 0.07	131 ± 4	2.21 ± 0.05	14.0 ± 0.4	2.30 ± 0.06
79.9	15.55	8.2 ± 0.2	2.64 ± 0.08	3.08 ± 0.08	138 ± 4	2.07 ± 0.05	14.0 ± 0.4	2.16 ± 0.06
84.9	14.92	7.6 ± 0.2	4.1 ± 0.1	3.42 ± 0.08	142 ± 4	1.89 ± 0.05	14.1 ± 0.4	2.05 ± 0.05
89.9	14.71	7.3 ± 0.2	5.7 ± 0.1	3.57 ± 0.09	146 ± 4	1.86 ± 0.05	14.4 ± 0.4	2.00 ± 0.05
100	7.59	—	—	4.2 ± 0.1	155 ± 4	1.52 ± 0.04	14.6 ± 0.4	1.85 ± 0.05

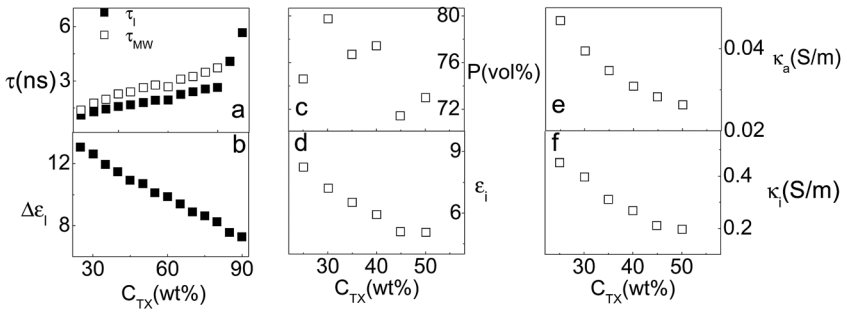

Fig. 4 The dependence of dielectric parameters (solid symbols) of low-frequency relaxation and phase parameters (open symbols) for the [bmim][BF_4]/TX-100 binary system on the weight concentration of TX-100 (C_{TX}): (a) experimental relaxation time τ_l and Maxwell–Wagner relaxation time τ_{MW}, (b) dielectric increment $\Delta\varepsilon_l$, (c) volume fraction of dispersed phase P, (d) permittivity of dispersed phase ε_i, (e) conductivity of continuous phase κ_a, (f) conductivity of dispersed phase κ_i.

observed C_{TX} is above the CMC of TX-100 in [bmim][BF_4], thus, we have reason to believe that the low-frequency relaxations of IL-based micelles/microemulsions contribute to the interfacial polarization. And the interesting thing is that the interfacial polarization was also found in micelles of TX-100 formed in water.[46] On basis of this conclusion, the phase parameters were calculated by the method introduced in Section 2.3, the results are shown in Fig. 4–6.

Fig. 4 also shows the variation of dielectric increment (of low-frequency relaxation) and phase parameters ($C_{TX} \leq 50.1\%$) of IL-based micelles as a function of C_{TX}. The phase parameters ($C_{TX} \geq 50.1\%$) are shown in Fig. S2 of the ESI.† As reported in part I of our work,[39] spherical micelles are only formed when $C_{TX} < 44.9\%$, this boundary concentration is near the concentration of the turning point (C_{TX} = 50.1%) observed in the dependence of phase parameters on C_{TX} as shown in Fig. S2a–d (ESI†) though there is not a turning point observed in the dependence of dielectric parameters on C_{TX} as shown in Fig. 4a and b. This phenomenon indicates that: on one hand, the Hanai theory which is used to calculate the phase parameters can be used only when $C_{TX} < 50.1\%$ because this theory only works for spherical particles; once above this concentration the phase parameters began to develop in the meaningless direction (Fig. S2a–d, ESI†), which means that this theory is no longer applicable because the non-spherical micelles are formed, and those data will no longer be discussed below. On the other hand, compared with dielectric parameters, the phase parameters can more precisely reflect the structural variation of IL-based micelles.

As shown in Fig. 4b, 5b and 6b, the magnitude of $\Delta\varepsilon_l$ (several to a dozen units) also conforms to the typical characteristic of interfacial polarization. As reported by O'Brein *et al.*[48,49] and Dukhin *et al.*,[50,51] the Maxwell–Wagner polarization should consider the particle surface and its double layers. The double layer of particles in IL-based micelles/microemulsions must be related to ILs because the electrostatic interactions between OE units of TX-100 locate the palisade layer of the particle surface and the imidazolium cation of the IL. Fig. 6b shows that $\Delta\varepsilon_l$ is proportional to the content of IL this proves that the low-frequency relaxation related to the content of the IL contributes to the formation of a double layer around the surface. Moreover, the decrease of the IL concentration may reduce the content of the IL in the double layer, and increase the volume fraction of particles (show in Fig. 4c and 6c) will reduce the effective particle charge due to the closeness of the counterion cloud.[52] These two factors have the same effect of reducing $\Delta\varepsilon_l$ as shown in Fig. 4b and 6b.

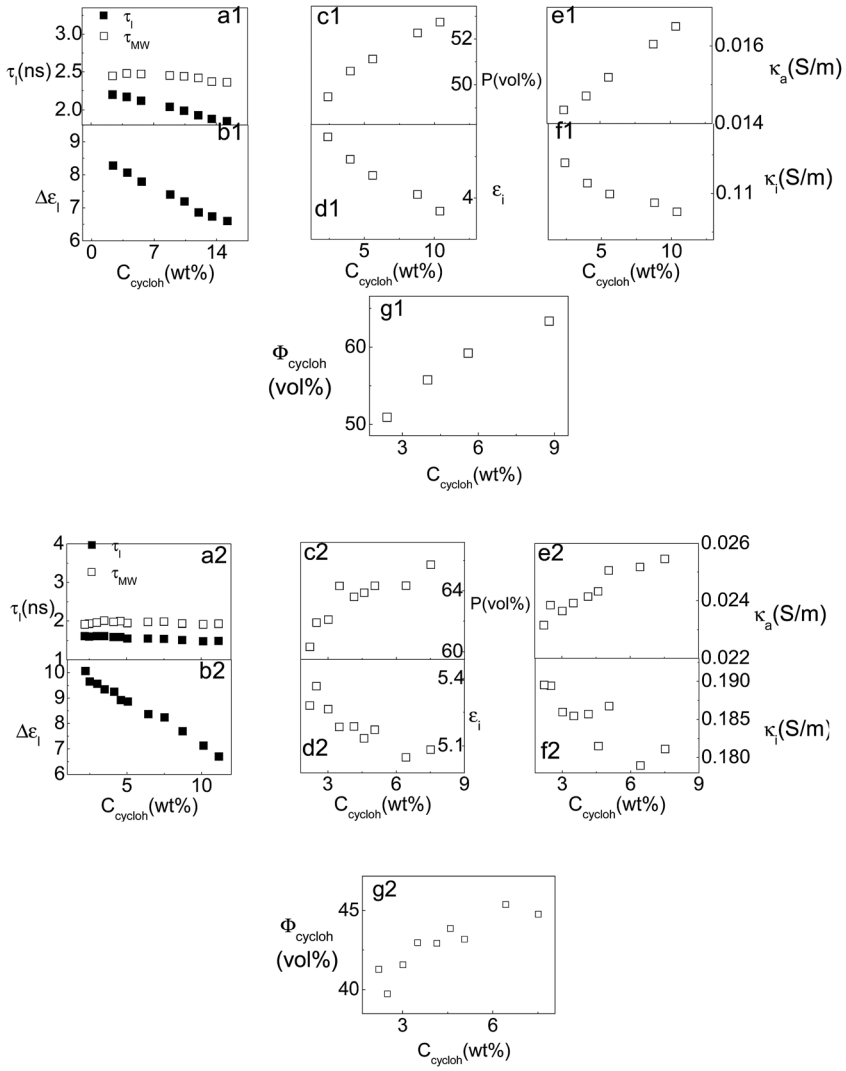

Fig. 5 The dependence of dielectric parameters of low-frequency relaxation and phase parameters of oil in IL micro-droplets (O/IL) of the [bmim][BF_4]/TX-100/cyclohexane ternary system on the weight concentration of cyclohexane (C_{cycloh}): (a) τ_l and τ_{MW}, (b) $\Delta\varepsilon_l$, (c) P, (d) ε_i, (e) κ_a, (f) κ_i and (g) volume fraction of cyclohexane in O/IL droplets (Φ_{cycloh}). Label 1 denotes the experimental path of IL-based microemulsion with a fixed weight ratio of IL/TX-100; label 2 denotes the experimental path of IL-based microemulsion with a fixed weight fraction of TX-100.

However, as for O/IL microemulsions, the above two factors have an opposite effect on the IL concentration dependence of $\Delta\varepsilon_l$. Obviously the former is the major influence factor, which is inferred from the decline of $\Delta\varepsilon_l$ as the content of the IL decreases as shown in Fig. 5b though P increases as shown in Fig. 5c.

Fig. 4c shows that the volume fraction of dispersed phase P in the concentration range of spherical particles fluctuates and its average value is relatively high (75.5%). The CMC of TX-100 in [bmim][BF_4] is very high (*circa* 0.33 mol L^{-1})[4] and the dispersed phase may include the ILs inserted into the TX-100 micelle phase,[19] which may be responsible for the computational deviation of Hanai theory in such a system.

The permittivity of TX-100 micelles dispersed in the IL (see Fig. 4d) is not in the range of pure TX-100 and pure [bmim][BF_4], but below the pure TX-100 expect the first concentration, and decreases with the increase of C_{TX}. This phenomenon states that the insertion of the IL into the micelle phase[19] may reduce the polarity of the whole micelles and decrease the content of the IL. As a result, the permittivity of the micelles reduces in the calculated concentration range. This, of course, also involved the computing deviation caused by the non-applicability of Hanai theory to this system. The situation is same as the data of Fig. 6d, where the dispersed phase is IL/O micro-droplets in the IL-based microemulsions.

Fig. 4e shows that the conductivity of the continuous phase κ_a decreases as C_{TX} increases. When micelles are once formed, κ_a becomes lower than that of the pure IL (0.74891 S m^{-1}), this is because the existence of the dispersed phase with a quite high volume fraction hindered the ion migration in the continuous phase, resulting in the speed of the ion transfer being less than that in the pure solvent (IL). Similar phenomena were also observed in other particle suspensions.[53,54] Moreover, an increase in the number of micelles will reduce the conductivity of the continuous phase as shown in Fig. 4e.

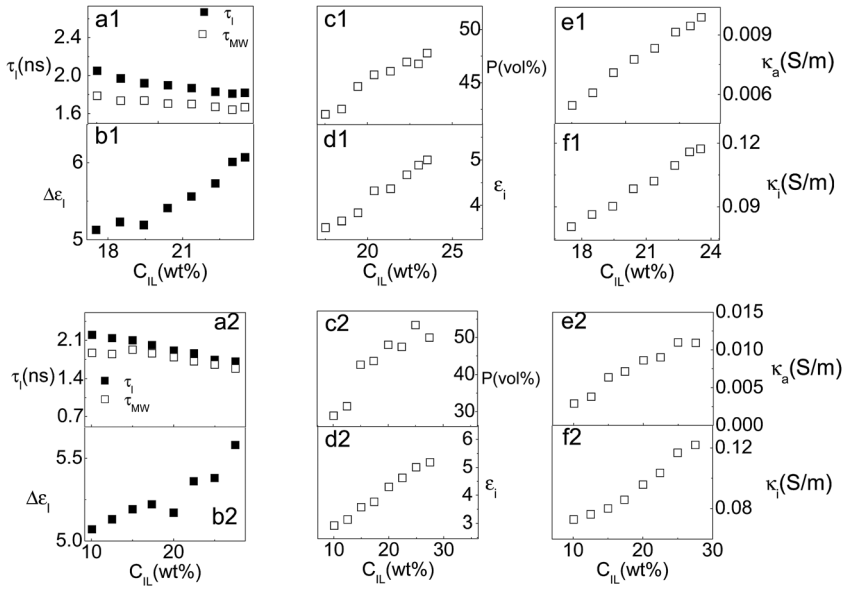

Fig. 6 The dependence of (a) τ_l and τ_{MW}, (b) $\Delta\varepsilon_l$, (c) P, (d) ε_i, (e) κ_a and (f) κ_i in oil in the IL sub-region (IL/O) of the [bmim][BF_4]/TX-100/cyclohexane ternary system on the weight concentration of the ionic liquid (C_{IL}). Label 1 denotes the experimental path of the IL-based microemulsion with a fixed weight ratio of IL/TX-100; label 2 denotes the experiment path of the IL-based microemulsion with a fixed weight fraction of TX-100.

The conductivity of the dispersed phase κ_i (0.45103) shown in Fig. 4f became very large once the micelles were formed, more than half of the pure IL solvent (0.74891), this is because the micelles contain a lot of IL molecules because of the insertion of ILs into the TX-100 micelle phase,[19] the number of imidazolium cations associated with every TX-100 molecule is approximately equal to eight as reported in our previous work.[39] Furthermore, when the content of ILs decreases, the ILs in micelles decrease, thus κ_i decreases.

4.3 Low-frequency relaxation mechanism and phase parameters of IL-based microemulsion

4.3.1 The sub-region contains oil-in-IL (O/IL) droplets. No matter whether the permittivity of the continuous phase substituted (ε_a) into Hanai theory is the static permittivity of the pure IL or the IL/TX-100 binary solvent, the value of ε_i is between the value of pure cyclohexane (1.99 at 35 °C) and pure TX-100 (7.59 as we measured), which indicates that the constituent of O/IL must contain TX-100, wherein TX-100 may be dissolved in the cyclohexane core to form the palisade layer on the surface of O/IL droplets. And the volume fraction of cyclohexane Φ_{cycloh} in the O/IL droplets can be estimated according to

$$\varepsilon_i = \Phi_{cycloh}\varepsilon_{cycloh} + (1 - \Phi_{cycloh})\varepsilon_{TX} \quad (9)$$

where we ignored the decrease effect of ε_a by the inclusion of TX-100 in O/IL droplets. On the basis of this calculation, when the pure IL serves as the continuous phase, the maximum value of Φ_{cycloh} (namely when P is maximum) is equal to 100.1% for the experimental path of the IL-based microemulsion with a fixed weight ratio of IL/TX-100. This means that O/IL droplets do not contain TX-100, which is in contrast with eqn (9). Thus, the continuous phase should be the IL/TX-100 binary solvent rather than the pure IL, and ε_a should be calculated by

$$\varepsilon_a = \Phi_{IL}\varepsilon_{IL} + \Phi_{TX}\varepsilon_{TX} \quad (10)$$

where the volume fractions of IL Φ_{IL} and TX-100 Φ_{TX} are calculated according to the weight ratio of IL/TX-100. The phase parameters of spherical oil droplets calculated in this situation are shown in Fig. 5c–f, and Φ_{cycloh} are shown in Fig. 5g, and the data in bicontinuous (B.C.) sub-regions are shown in Fig. S2e–n (ESI†). Moreover, the largest value of Φ_{cycloh} is 63.35% (Fig. 5g1) or 45.38% (Fig. 5g2), which is reasonable because it means that TX-100 is contained in O/IL droplets. Besides, an increase in Φ_{cycloh} when C_{cycloh} increases is also reasonable as shown in Fig. 5g. The error of ε_a is −6.0 to −2.5% when TX-100 contained in O/IL droplets is excluded from the continuous phase, thus the decline effect caused by TX-100 in O/IL for ε_a can be ignored. In other words, calculating the phase parameters using binary solvent permittivity as ε_a is reasonable approximately. The situation is the same for the IL/O microemulsion region as introduced in the next section.

As shown in Fig. S2e (ESI†), with the increase of C_{cycloh}, P first increases and then decreases, which indicates that the concentration of the highest point is the critical percolation concentration because this concentration is in accord with the boundary concentration between O/IL and B.C. sub-regions as reported in the literature.[7] As shown in Fig. 5c, the increase of P with the increase of C_{cycloh} is because the number and volume of O/IL micro-droplets increase. In the smallest concentration P is fairly high (49.48%) and rapidly increases to 52.74%, this phenomenon conforms to the prediction of the phase diagram[7] in which the area of the O/IL region is very narrow and rapidly enters the B.C. region with increasing C_{cycloh}. The last three points of P in Fig. S2e (ESI†) decrease rather than increasing

when C_{cycloh} increases suggesting that the spherical droplets change into the B.C. structure and the Hanai theory is not applicable to calculate the phase parameters anymore in these concentration regions, this conclusion is supported by the literature.[7]

The conductivity of the continuous phase (κ_a) shown in Fig. 5e is less than that of the pure IL because the binary solvent is used as the continuous phase and a lot of O/IL droplets exist in the continuous phase with a high volume fraction. Although the volume fraction of TX-100 decreases with the increase of C_{cycloh} as shown in Fig. 5g, the volume fraction of O/IL droplets increases as shown in Fig. 5c, which means more and more TX-100 turn into O/IL droplets from the continuous phase, namely the concentration of the IL in the continuous phase increases, thus κ_a in Fig. 5e increases as C_{cycloh} increases. The conductivity of the dispersed phase (κ_i) in Fig. 5f is higher than that of the continuous phase because ILs insert into the TX-100 palisade layer of the O/IL droplets. The increase of the cyclohexane volume fraction in the O/IL droplets (Fig. 5g) results in the decrease of κ_i as C_{cycloh} increases (Fig. 5f).

4.3.2 IL-in-Oil (IL/O) microemulsion sub-region. As the transitional region between O/IL and IL/O regions, the B.C. region does not have a spherical particle structure and has a double channel structure (oil channels and IL channels) instead, but the double layer may still exist on the surface wall of these channels. As we concluded in Section 4.2, the observed low-frequency relaxation of O/IL and IL/O droplets should be caused by the Maxwell–Wagner polarization, more specifically this polarization for suspensions is ascribed to the fluctuation of space charge (arising in solution neighboring to the particle surface) within the Debye length (a measure of the thickness of double layer characterizing the size of the diffuse ion cloud). In the B.C. region, the double layer still exists and then the Debye lengths still exist, that is why the low-frequency relaxation is still observed in the B.C. region as shown in Fig. 5a, b and 6a, b. The situation is similar in un-spherical micelles (namely when $C_{TX} > 50.1\%$) in Fig. 4a and b.

In the IL/O region for the experimental path of IL/O microemulsion with a fixed weight ratio of IL/TX-100, according to the Hanai theory, when ε_a is substituted by the static dielectric constant of pure cyclohexane, the obtained value of ε_i is around 10^{11} and τ_{MW} and κ_i are both negative. At the same time, in the experimental path with a fixed weight fraction of TX-100, κ_i is also negative if the static permittivity of pure cyclohexane is used as ε_a, and τ_{MW} is one order smaller than τ_l. Thus, similar with the O/IL region, ε_a of IL/O microemulsion should be the value of binary solvent calculated by eqn (11) rather than that of pure cyclohexane, whose value can be calculated as

$$\varepsilon_a = \Phi_{cycloh}{}'\varepsilon_{cycloh} + \Phi_{TX}{}'\varepsilon_{TX} \quad (11)$$

where the volume fractions of cyclohexane $\Phi_{cycloh}{}'$ and TX-100 $\Phi_{TX}{}'$ in the IL/O region are calculated according to the weight ratio between cyclohexane and TX-100 for both of the experimental paths. The phase parameters calculated in this situation are shown in Fig. 6c–f.

One can see from Fig. 6c that P increases with the increase of C_{IL}, this is because the number and volume of IL/O microdroplets increases. As shown in Fig. 6c1, in the smallest concentration P is fairly high (42.02%) and rapidly increases to 47.77%, which agrees with the prediction of the phase diagram[7] that the area of IL/O is very narrow and rapidly enters the B.C. phase with the increase of C_{IL}. On the other hand, for the experimental path with a fixed weight ratio of IL/TX-100 (Fig. 6c1), when C_{IL} decreases, P decreases rapidly suggesting that the IL/O structure will be destroyed because, comparatively speaking, the decrease speed of the TX-100 content is greater than that of the IL content, there is not enough TX-100 molecules to build the palisade layer of IL/O droplets which can dissociate oil from the IL, that is to say the samples will enter the two phase region, which is consistent with the phase diagram reported in the literature.[7] And for the experimental path with a fixed weight fraction of TX-100 (Fig. 6c2), when the content of cyclohexane increases, because the content of TX-100 does not change and the content of the IL reduces, the IL/O disappeared and reverse micelles (where the IL was inserted into) are formed instead, that is why it does not enter the two phase region as shown in the phase diagram.[7]

As shown in Fig. 6d, ε_i is below that of pure TX-100, this is because of the reduction of polarity of IL/O droplets by the insertion of the IL into the palisade layer and the dissolution of TX-100 in the IL core, being the same as discussed for the data in Fig. 4d in Section 4.2.

The IL will more or less interfuse into the continuous phase and will increase with the increase of the IL concentration, thus the conductivity of the continuous phase will increase a little as shown in Fig. 6e. Moreover, the conductivity of the continuous phase in the IL/O region (Fig. 6e) is smaller than that in the O/IL region (Fig. 5e) because the continuous phase shown in Fig. 6e is oil. Due to the core of the droplets being formed by the IL, the conductivity of the dispersed phase shown in Fig. 6f is bigger than the conductivity of continuous phase shown in Fig. 6e.

5. Conclusions

In this work, we made dielectric measurements for [bmim][BF_4]/TX-100 binary systems and [bmim][BF_4]/TX-100/cyclohexane ternary systems over a frequency range from 40 Hz to 20 GHz, and analyzed the spectra theoretically by interfacial polarization theory. The analysis of the dielectric spectra mainly focused on the polarization mechanism of the observed low-frequency dielectric relaxation, which is located at 100 MHz. The dielectric properties of self-organization systems of surfactant molecules formed within the ionic liquid and some information about the interfacial polarization are first revealed. These findings may help to supplement the knowledge of such systems.

The low-frequency dielectric relaxations are modeled by a cole–cole term, and the dielectric parameters were obtained. For both binary and ternary systems, according to the relaxation times calculated by the Hanai equation based on the

Maxwell–Wagner theory, the low-frequency relaxation contributes to the interfacial polarization. Moreover, various factors (such as the linear dependence of dielectric increment on the content of ionic liquid and low-frequency relaxations that are also observed in the B.C. sub-region whose relaxation time continuously changes from the values in the IL/O sub-region to the O/IL sub-region) indicate that ionic liquids existing in double layers of the surface may play an important role in this interfacial polarization.

The phase parameters of IL-based micelles/microemulsions, such as the permittivity and conductivity of continuous and dispersed phases and the volume fraction of the dispersed phase, were obtained using the Hanai equation and the corresponding analytical method. As far as we know this is the first time these phase parameters which reflect the internal properties of the constituent phases in these self-organization systems of surfactant molecules formed within an IL were provided. The addition of a lot of surfactant makes the permittivity of continuous phase should take the value of binary solvent (TX-100/cyclohexane and TX-100/IL) rather than that of pure solvent (cyclohexane and IL), and volume fractions of dispersed phases are considerably high both in micelles, IL/O and O/IL microemulsions. On the other hand, the insertion of ILs into the interface palisade layer of micelles/microemulsions has an enormous implication on the phase parameters of these systems, namely a fairly low permittivity and a relatively high conductivity of the dispersed phase. It is worth mentioning that the volume fraction of cyclohexane in O/IL droplets is given quantitatively, which is of importance for the quantitative research of the microstructure of IL-based microemulsions. We also discussed the rationality of phase parameters and their dependencies on the composition. These phase parameters provide necessary electrical parameters for modeling these systems.

Conflicts of interest

There are no conflicts to declare.

Acknowledgements

The authors wish to thank Jinmei Pan and Shaojie Zhao for helpful measurement of high frequency data. Financial support of this work by the National Natural Science Foundation of China (No. 21403051, 21173025, 21673002 and 21473012) is gratefully acknowledged.

References

1 T. L. Merrigan, E. D. Bates, S. C. Dorman and J. H. Davis, New fluorous ionic liquids function as surfactants in conventional room-temperature ionic liquids, *Chem. Commun.*, 2000, 2051–2052.

2 Y. Ma and T. P. Lodge, Poly(methyl methacrylate)-*block*-poly(*n*-butyl methacrylate) diblock copolymer micelles in an ionic liquid: scaling of core and corona size with core block length, *Macromolecules*, 2016, **49**(9), 3639–3646.

3 K. A. Fletcher and S. Pandey, Surfactant aggregation within room-temperature ionic liquid 1-ethyl-3-methylimidazolium bis (trifluoromethylsulfonyl)imide, *Langmuir*, 2004, **20**(1), 33–36.

4 Y. A. Gao, N. Li, X. W. Li, S. H. Zhang, L. Q. Zheng, X. T. Bai and L. Yu, Microstructures of micellar aggregations formed within 1-butyl-3-methylimidazolium type ionic liquids, *J. Phys. Chem. B*, 2009, **113**(1), 123–130.

5 S. Palchowdhury and B. L. Bhargava, Glycine molecules in ionic liquid based reverse micelles: investigation of structure and dynamics using molecular dynamics simulations, *J. Mol. Liq.*, 2017, **230**, 384–394.

6 T. L. Greaves and C. J. Drummond, Ionic liquids as amphiphile self-assembly media, *Chem. Soc. Rev.*, 2008, **37**(8), 1709–1726.

7 H. X. Gao, J. C. Li, B. X. Han, W. N. Chen, J. L. Zhang, R. Zhang and D. D. Yan, Microemulsions with ionic liquid polar domains, *Phys. Chem. Chem. Phys.*, 2004, **6**(11), 2914–2916.

8 J. Li, J. Zhang, B. Han, Y. Wang and L. Gao, Compressed CO_2-enhanced solubilization of 1-butyl-3-methylimidazolium tetrafluoroborate in reverse micelles of Triton X-100, *J. Chem. Phys.*, 2004, **121**(15), 7408–7412.

9 Y. Gao, J. Zhang, H. Xu, X. Zhao, L. Zheng, X. Li and L. Yu, Structural studies of 1-butyl-3-methylimidazolium tetrafluoroborate/TX-100/*p*-xylene ionic liquid microemulsions, *ChemPhysChem*, 2006, **7**(7), 1554–1561.

10 N. Li, Y. A. Gao, L. Q. Zheng, J. Zhang, L. Yu and X. W. Li, Studies on the micropolarities of bmimBF_4/TX-100/toluene ionic liquid microemulsions and their behaviors characterized by UV-visible spectroscopy, *Langmuir*, 2007, **23**(3), 1091–1097.

11 Y. Gao, N. Li, L. Zheng, X. Zhao, J. Zhang, Q. Cao, M. Zhao, Z. Li and G. Zhang, The effect of water on the microstructure of 1-butyl-3-methylimidazolium tetrafluoroborate/TX-100/benzene ionic liquid microemulsions, *Chem. – Eur. J.*, 2007, **13**(3), 2661–2670.

12 J. Eastoe, S. Gold, S. E. Rogers, A. Paul, T. Welton, R. K. Heenan and I. Grillo, Ionic liquid-in-oil microemulsions, *J. Am. Chem. Soc.*, 2005, **127**(20), 7302–7303.

13 X. Yu, Q. Li, M. Wang, N. Du and X. Huang, Study on the catalytic performance of laccase in the hydrophobic ionic liquid-based bicontinuous microemulsion stabilized by polyoxyethylene-type nonionic surfactants, *Soft Matter*, 2016, **12**(6), 1713–1720.

14 Y. Gao, N. Li, L. Zheng, X. Bai, L. Yu, X. Zhao, J. Zhang, M. Zhao and Z. Li, Role of solubilized water in the reverse ionic liquid microemulsion of 1-butyl-3-methylimidazolium tetrafluoroborate/TX-100/benzene, *J. Phys. Chem. B*, 2007, **111**(10), 2506–2513.

15 Y. A. Gao, S. B. Han, B. X. Han, G. Z. Li, D. Shen, Z. H. Li, J. M. Du, W. G. Hou and G. Y. Zhang, TX-100/water/1-butyl-3-methylimidazolium hexafluorophosphate microemulsions, *Langmuir*, 2005, **21**(13), 5681–5684.

16 J. H. Porada, D. Zauser, B. Feucht and C. Stubenrauch, Tailored ionic liquid-based surfactants for the formation of microemulsions with water and a hydrophobic ionic liquid, *Soft Matter*, 2016, **12**, 6352–6356.

17 J. Kuchlyan and N. Kundu, Ionic liquids in microemulsions: formulation and characterization, *Curr. Opin. Colloid Interface Sci.*, 2016, **25**, 27–38.

18 N. Anjum, M.-A. Guedeau-Boudeville, C. Stubenrauch and A. Mourchid, Phase behavior and microstructure of microemulsions containing the hydrophobic ionic liquid 1-butyl-3-methylimidazolium hexafluorophosphate, *J. Phys. Chem. B*, 2009, **113**(1), 239–244.

19 K. Behera, P. Dahiya and S. Pandey, Effect of added ionic liquid on aqueous triton X-100 micelles, *J. Colloid Interface Sci.*, 2007, **307**(1), 235–245.

20 R. Pramanik, S. Sarkar, C. Ghatak, V. G. Rao and N. Sarkar, Ionic liquid containing microemulsions: probe by conductance, dynamic light scattering, diffusion-ordered spectroscopy NMR measurements, and study of solvent relaxation dynamics, *J. Phys. Chem. B*, 2011, **115**(10), 2322–2330.

21 V. G. Rao, C. Banerjee, S. Ghosh, S. Mandal, J. Kuchlyan and N. Sarkar, A step toward the development of high-temperature stable ionic liquid-in-oil microemulsions containing double-chain anionic surface active ionic liquid, *J. Phys. Chem. B*, 2013, **117**(24), 7472–7480.

22 C. Banerjee, N. Kundu, S. Ghosh, S. Mandal, J. Kuchlyan and N. Sarkar, Fluorescence resonance energy transfer in microemulsions composed of tripled-chain surface active ionic liquids, RTILs, and biological solvent: an excitation wavelength dependence study, *J. Phys. Chem. B*, 2013, **117**(32), 9508–9517.

23 *Ionic Liquids in Synthesis*, ed. P. Wasserscheid and T. Welton, Wiley-VCH, Weinheim, Germany, 2003.

24 B. Dong, S. Zhang, L. Zheng and J. Xu, Ionic liquid microemulsions: a new medium for electropolymerization, *J. Electroanal. Chem.*, 2008, **619-620**, 193–196.

25 B. Dong, J. Xu, L. Zheng and J. Hou, Electrodeposition of conductive poly(3-methoxythiophene) in ionic liquid microemulsions, *J. Electroanal. Chem.*, 2009, **628**(1-2), 60–66.

26 Y. W. Sun, K. Q. Yan and X. R. Huang, Formation, characterization and enzyme activity in water-in-hydrophobic ionic liquid microemulsion stabilized by mixed cationic/nonionic surfactants, *Colloids Surf., B*, 2014, **122**, 66–71.

27 R. Barchini and R. Pottel, Counterion contribution to the dielectric spectrum of aqueous solutions of ionic surfactant micelles, *J. Phys. Chem.*, 1994, **98**(32), 7899–7905.

28 J. Oizumi, H. Furusawa, Y. Kimura and K. Ito, High-frequency dielectric relaxation of linear micelles in aqueous solutions of cetyltrimethylammonium bromide with sodium salicylate, *Langmuir*, 1997, **13**(11), 3052–3054.

29 C. Baar, R. Buchner and W. Kunz, Dielectric relaxation of cationic surfactants in aqueous solution. 2. Solute relaxation, *J. Phys. Chem. B*, 2001, **105**(15), 2914–2922.

30 C. Cametti, Dielectric spectra of ionic water-in-oil microemulsions below percolation: frequency dependence behavior, *Phys. Rev. E: Stat., Nonlinear, Soft Matter Phys.*, 2010, **81**(3), 031403.

31 R. Wipf, S. Jaksch and B. Stühn, Dynamics in water-AOT-*n*-decane microemulsions with poly(ethylene glycol) probed by dielectric spectroscopy, *Colloid Polym. Sci.*, 2010, **288**(5), 589–601.

32 K. J. He, K. S. Zhao, J. L. Chai and G. Z. Li, Dielectric analysis of the APG/*n*-butanol/cyclohexane/water nonionic microemulsions, *J. Colloid Interface Sci.*, 2007, **313**(2), 630–637.

33 C. Daguenet, P. J. Dyson, I. Krossing, A. Oleinikova, J. Slattery, C. Wakai and H. Weingärtner, Dielectric response of imidazolium-based room-temperature ionic liquids, *J. Phys. Chem. B*, 2006, **110**(25), 12682–12688.

34 A. Stoppa, J. Hunger, R. Buchner, G. Hefter, A. Thoman and H. Helm, Interactions and dynamics in ionic liquids, *J. Phys. Chem. B*, 2008, **112**(16), 4854–4858.

35 K. Nakamura and T. Shikata, Systematic dielectric and NMR study of the ionic liquid 1-alkyl-3-methyl imidazolium, *ChemPhysChem*, 2010, **11**(1), 285–294.

36 J. Hunger, A. Stoppa, R. Buchner and G. Hefter, From ionic liquid to electrolyte solution: dynamics of 1-*N*-butyl-3-*N*-methylimidazolium tetrafluoroborate/dichloromethane mixtures, *J. Phys. Chem. B*, 2008, **112**(41), 12913–12919.

37 C. Schröder, J. Hunger, A. Stoppa, R. Buchner and O. Steinhauser, On the collective network of ionic liquid/water mixtures. II. Decomposition and interpretation of dielectric spectra, *J. Chem. Phys.*, 2008, **129**(18), 184501.

38 G. Dimitrakis, I. J. Villar-Garcia, E. Lester, P. Licence and S. Kingman, Dielectric spectroscopy: a technique for the determination of water coordination within ionic liquids, *Phys. Chem. Chem. Phys.*, 2008, **10**, 2947–2951.

39 Y. W. Lian and K. S. Zhao, Dielectric analysis of micelles and microemulsions formed in a hydrophilic ionic liquid. I. Interaction and percolation, *J. Phys. Chem. B*, 2011, **115**(39), 11368–11374.

40 Y. W. Lian and K. S. Zhao, Study of micelles and microemulsions formed in a hydrophobic ionic liquid by a dielectric spectroscopy method. I. Interaction and percolation, *Soft Matter*, 2011, **7**(19), 8828–8837.

41 D. V. Blackham and R. D. Pollard, An improved technique for permittivity measurements using a coaxial pobe, *IEEE Trans. Instrum. Meas.*, 1997, **46**(5), 1093–1099.

42 K. S. Cole and R. H. Cole, Dispersion and absorption in dielectrics I. Alternating current characteristics, *J. Chem. Phys.*, 1941, **9**(4), 341–351.

43 K. W. Wagner, Erklärung der dielektrischen Nachwirkungsvorgänge auf Grund Maxwellscher Vorstellungen, *Arch. Electrotech.*, 1914, **2**(9), 371–387.

44 D. A. G. Bruggeman, Berechnung verschiedener physikalischer Konstanten von heterogenen Substanzen. I. Dielektrizitätskonstanten und Leitfähigkeiten der Mischkörper aus isotropen Substanzen, *Ann. Phys.*, 1935, **416**(7), 636–664.

45 T. Hanai, A. Ishikawa and N. Koizumi, Systematic analysis to determine the dielectric phase parameters from dielectric relaxations caused by diphasic structure of disperse systems, *Bull. Inst. Chem. Res., Kyoto Univ.*, 1977, **55**(4), 376–393.

46 K. Asami, Dielectric properties of water in Triton X-100 (nonionic detergent)–water mixtures, *J. Phys.: Condens. Matter*, 2007, **19**, 376102.

47 T. L. Chelidze and Y. Gueguen, Electrical spectroscopy of porous rocks: a review-I. Theoretical models, *Geophys. J. Int.*, 1999, **137**(1), 1–15.

48 R. W. O'Brien, The high-frequency dielectric dispersion of a colloid, *J. Colloid Interface Sci.*, 1986, **113**(1), 81–93.
49 R. W. O'Brein, The response of a colloidal suspension to an alternating electric field, *Adv. Colloid Interface Sci.*, 1982, **16**(1), 281–320.
50 S. S. Dukhin, Electrochemical characterization of the surface of a small particle and nonequilibrium electric surface phenomena, *Adv. Colloid Interface Sci.*, 1995, **61**, 17–49.
51 S. S. Dukin and V. N. Shilov, *Dielectric phenomena and the double layer in disperse system and polyelectrolytes*, Wiley, New York, 1974.
52 R. Barchini and D. A. Saville, Dielectric response measurements on concentrated colloidal dispersions, *J. Colloid Interface Sci.*, 1995, **173**(1), 86–91.
53 S. Levine and G. H. Neale, The prediction of electrokinetic phenomena within multiparticle systems. I. Electrophoresis and electroosmosis, *J. Colloid Interface Sci.*, 1974, **47**(2), 520–529.
54 J. K. Huan and T. H. Wen, Electric conductivity of a suspension of charged colloidal spheres with thin but polarized double layers, *Colloid Polym. Sci.*, 2002, **280**(10), 922–928.